



CHORUS

This is the accepted manuscript made available via CHORUS. The article has been published as:

Impurity quantum phase transition in a current-carrying d-wave superconductor

Hua Chen, Yezheng Wu, Shuxiang Yang, Jianhui Dai, and Jian-Xin Zhu

Phys. Rev. B **85**, 205139 — Published 29 May 2012

DOI: [10.1103/PhysRevB.85.205139](https://doi.org/10.1103/PhysRevB.85.205139)

Impurity Quantum Phase Transition in a Current-Carrying d -Wave Superconductor

Hua Chen,¹ Yezheng Wu,¹ Shuxiang Yang,² Jianhui Dai,^{3,1} and Jian-Xin Zhu⁴

¹Zhejiang Institute of Modern Physics, Zhejiang University, Hangzhou 310027, China

²Department of Physics and Astronomy, Louisiana State University, Baton Rouge, Louisiana 70803, USA

³Condensed Matter Group, Department of Physics,

Hangzhou Normal University, Hangzhou 310036, China

⁴Theoretical Division, Los Alamos National Laboratory, Los Alamos, New Mexico 87545, USA

(Dated: May 16, 2012)

We study an Anderson impurity embedded in a d -wave superconductor carrying a supercurrent. The low-energy impurity behavior is investigated by using the numerical renormalization group method developed for arbitrary electronic bath spectra. The results explicitly show that the local impurity state is completely screened upon the non-zero current intensity. The impurity quantum criticality is in accordance with the well-known Kosterlitz-Thouless transition.

PACS numbers: 71.10.Hf, 71.27.+a, 75.20.Hr, 71.28.+d

I. INTRODUCTION

The behavior of a single magnetic impurity in correlated electron systems has attracted intensive interest in condensed matter physics.¹ While the problem is well studied when the host is a simple metal,² the correlations among the host electrons may lead to much complicated impurity behavior deviating from the Fermi liquid properties.¹ Specifically, the Kondo screened state, i.e., an entanglement state between the impurity spin and a conduction electron, may become unstable at zero temperature upon the depletion of the density of states (DOS) at the Fermi levels, or the change of certain nonthermal parameters. Such kind of impurity quantum phase transition (IQPT) may take place in metallic systems with a pseudo gap.³ The response of a known impurity behavior upon the change of effective couplings could provide important information of the host itself, and thus can be used to probe the ground state and low-energy physics of the host electrons.⁴ On the other hand, within a known host, the different response of a quantum impurity with internal dynamical degrees of freedom versus a static impurity, to an external control parameter, may shed insight on the role played by a doped impurity in a correlated electron medium,^{5,6} which is a relatively rarely explored area. In this Article, we study the property of an Anderson impurity embedded in a d -wave superconductor. Our analysis, based on the numerical renormalization group (NRG) method, unambiguously shows that an IQPT of the Kosterlitz-Thouless type can be induced in a d -wave superconductor carrying non-zero persistent currents. This means that the Kondo temperature increases with the current q exponentially, $T_K \propto e^{-\alpha/q}$, with α being a parameter linearly dependent on the Coulomb interaction of the impurity orbital. The obtained results can be tested by scanning tunneling microscopy (STM), which has been used to measure the local electronic structure around a doped impurity in conventional⁷ and unconventional superconductors⁸ in the absence of a current flow.

The outline of this paper is as follows. In Sec. II, we introduce a model system to describe an Anderson im-

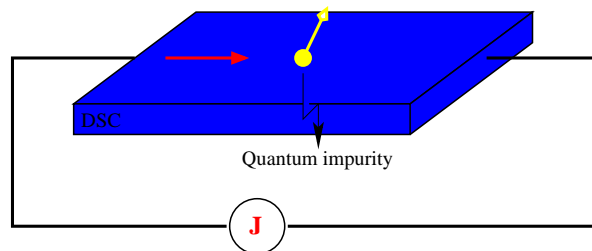


FIG. 1: (Color online) An Anderson impurity embedded in a two-dimensional d -wave superconductor. A supercurrent \mathbf{J} is fed into the superconductor from a current source. The local electron structure around the impurity can be measured by scanning tunneling microscopy.

purity in a current carrying d -wave superconductor. We present the formulation for calculating the quasiparticle spectrum of the superconducting bath in the presence of the supercurrent. The NRG approach is then introduced to solve the quantum impurity problem. In Sec. III, we present numerical results and identify the nature of the IQPT. Finally, concluding remarks are given in Sec. IV.

II. MODEL AND METHOD

It is now well accepted that high-temperature cuprate superconductors exhibit a d -wave pairing symmetry.⁹ These materials have a two-dimensional layered structure. In their thin film form, a supercurrent can be injected by a current source, as shown schematically in Fig. 1. We notice that a persistent current can also be generated by piercing a magnetic flux through the axial of a mesoscopic hollow superconducting cylinder, due to the Aharonov-Bohm effect.¹⁰ The flux driven current is negligibly small in the thermodynamic limit. As such, the setup proposed here is more suitable for the study of quantum impurity problem in an unconventional fermionic bath, and should be experimentally accessible.

We model the problem by the following Hamiltonian

$$\mathcal{H} = \mathcal{H}_{\text{BCS}} + \mathcal{H}_{\text{imp}} + \mathcal{H}_{\text{hybrid}}, \quad (1)$$

where $\mathcal{H}_{\text{BCS}} = \sum_{\mathbf{k},\sigma} \xi_{\mathbf{k}+\mathbf{q}} c_{\mathbf{k}\sigma}^\dagger c_{\mathbf{k}\sigma} + \sum_{\mathbf{k}} [\Delta_{\mathbf{k}} c_{\mathbf{k}\uparrow}^\dagger c_{-\mathbf{k}\downarrow}^\dagger + \text{h.c.}]$, $\mathcal{H}_{\text{imp}} = \sum_{\sigma} \epsilon_d d_{\sigma}^\dagger d_{\sigma} + U n_{d\uparrow} n_{d\downarrow}$, and $\mathcal{H}_{\text{hybrid}} = \frac{1}{\sqrt{N_L}} \sum_{\mathbf{k},\sigma} [V_{\mathbf{k}} c_{\mathbf{k}\sigma}^\dagger d_{\sigma} + \text{h.c.}]$. Here $c_{\mathbf{k}\sigma}$ annihilates one conduction electron of momentum \mathbf{k} and spin projection σ , while d_{σ} annihilates one localized d -electron of spin projection σ . In the tight-binding approximation, the conduction electrons have the normal and d -wave superconducting gap dispersions, $\xi_{\mathbf{k}} = -2t(\cos k_x + \cos k_y) - 4t' \cos k_x \cos k_y - \mu$ and $\Delta_{\mathbf{k}} = (\Delta_0/2)(\cos k_x - \cos k_y)$, respectively. The center-of-mass momentum, $2\mathbf{q}$, of a Cooper pair determines the current flow.¹¹ Note that the BCS superconducting part of the Hamiltonian is written in an unconventional way. We have transferred the momentum $2\mathbf{q}$ shift on the Cooper pair wavefunction onto the momentum \mathbf{q} shift on the single-particle kinetic energy via a local gauge transformation in real space. A detailed derivation is given in Appendix A. Other parameters ϵ_d , U , and $V_{\mathbf{k}}$ are the localized level, the on-site Coulomb interaction, and the impurity coupling, respectively. N_L is the number of lattice sites.

The quasiparticle density of states of the 2D current-carrying d -wave superconductor can be found by diagonalizing \mathcal{H}_{BCS} via the formula

$$\rho(\omega) = \frac{1}{N_L} \sum_{\mathbf{k}} [|u_{\mathbf{k},\mathbf{q}}|^2 \delta(\omega - E_{\mathbf{k},\mathbf{q}}^+) + |v_{\mathbf{k},\mathbf{q}}|^2 \delta(\omega - E_{\mathbf{k},\mathbf{q}}^-)], \quad (2)$$

where $E_{\mathbf{k},\mathbf{q}}^{\pm} = Z_{\mathbf{k},\mathbf{q}} \pm [Q_{\mathbf{k},\mathbf{q}}^2 + \Delta_{\mathbf{k}}^2]^{1/2}$, with $Z_{\mathbf{k},\mathbf{q}} = (\xi_{\mathbf{k}+\mathbf{q}} - \xi_{\mathbf{k}-\mathbf{q}})/2$ and $Q_{\mathbf{k},\mathbf{q}} = (\xi_{\mathbf{k}+\mathbf{q}} + \xi_{\mathbf{k}-\mathbf{q}})/2$. The electron- and hole components of the Bogoliubov-de Gennes eigenfunction are given by $|u(v)_{\mathbf{k},\mathbf{q}}|^2 = [1 \pm Q_{\mathbf{k},\mathbf{q}}/E_{\mathbf{k},\mathbf{q}}^0]/2$ with $E_{\mathbf{k},\mathbf{q}}^0 = [Q_{\mathbf{k},\mathbf{q}}^2 + \Delta_{\mathbf{k}}^2]^{1/2}$.

In order to solve the whole problem, we generalize the NRG method^{2,18} to study the impurity properties with an arbitrary form of the DOS. It is sufficient for our purpose to take into account the coupling between the impurity spin and the particle-excitations. The latter is the only necessary ingredient in d -wave superconductors.^{19,20} We therefore ignore the anomalous part and just study a modified Anderson model with the impurity coupled to the electron-like excitation spectrum. As such, we use the following Hamiltonian to the derivation of the NRG equations:^{16,21}

$$\begin{aligned} \mathcal{H} = & \mathcal{H}_{\text{imp}} + D \sum_{\sigma} \int_{-1}^1 d\varepsilon g(\varepsilon) a_{\varepsilon\sigma}^\dagger a_{\varepsilon\sigma} \\ & + D \sum_{\sigma} \int_{-1}^1 d\varepsilon h(\varepsilon) (d_{\sigma}^\dagger a_{\varepsilon\sigma} + a_{\varepsilon\sigma}^\dagger d_{\sigma}), \end{aligned} \quad (3)$$

where we introduced a one-dimensional energy representation for the particle-like excitations $a_{\varepsilon\sigma}^\dagger$ with the scaled energy ε and the band-cutoffs at $\pm D$. $g(\varepsilon)$ and $h(\varepsilon)$ are the energy dispersion and hybridization self-consistently defined by $\rho(\varepsilon)$ and $V_{\mathbf{k}}$ respectively as in Ref. 21.

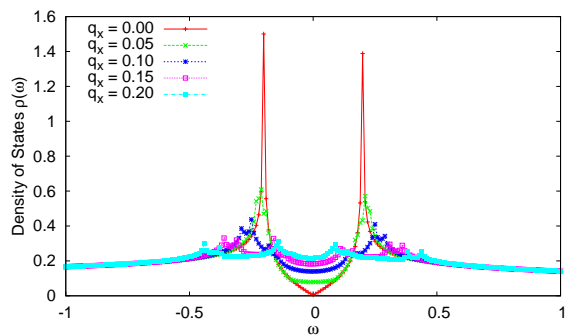


FIG. 2: (Color online) Density of states as a function of energy for various values of drift momentum q_x .

III. NUMERICAL RESULTS

In the numerical calculations, we take $t = 1$, $t' = -0.2$, $\mu = -0.78$, $\Delta_0 = 0.2$. The energy is measured in units of $t = 1$ unless specified otherwise. Without loss of generality, we take $\mathbf{q} = (q_x, q_y) = (q_x, 0)$. In Fig. 2, we show the DOS as a function of energy for various values of q_x . A small intrinsic lifetime broadening $\Gamma = 10^{-3}$, and the lattice sites of 5000×5000 are chosen. In the absence of the current, the calculated DOS vanishes linearly as expected, and the finite size effect on the DOS is negligible as shown in the Appendix B. It increases around the Fermi energy as a response to the non-zero current.

To handle the *arbitrary* $\rho(\omega)$, we follow the generic scheme of Ref. 21 to discretize the Hamiltonian given by Eq. (3), and then solve it by the NRG for different values of U and \mathbf{q} at the symmetric point $\epsilon_d = -U/2$, with the RG parameter $\Lambda = 2$. At each iteration step we keep about 1500 states, depending on the quantities calculated, and the total number of iterations is $N_{\text{max}} = 100$. Throughout the work, a value of the band cut-off $D = 1$ is chosen.

Distinct from the case of either a wide-band normal metal with a constant DOS, where the impurity spin being in a strong coupling (SC) limit, or a conventional s -wave superconductor with a hard-gap everywhere on the Fermi surface, where the impurity spin being in the local moment (LM) limit, the existence of nodal zero-energy quasiparticles in a d -wave superconductor^{4,9} has a non-trivial implication to the fate of quantum impurity states. Earlier studies by taking the DOS with a soft-gap, $\rho(\omega) \sim |\omega|^r$ ($r = 1$ for the d -wave superconductor), have shown the existence of a critical coupling, separating the LM and SC phases.^{3,12-16} The present model is more intriguing, as the low-energy excitations in a d -wave superconductor can readily be proliferated by pumping in a supercurrent, which should have a significant control of the impurity state.¹⁷ The purpose of the present work is to demonstrate that a Kosterlitz-Thouless-like IQPT can be realized by tuning the (super-)current.

In the absence of the current, the impurity in the present symmetric Anderson model should be in the LM

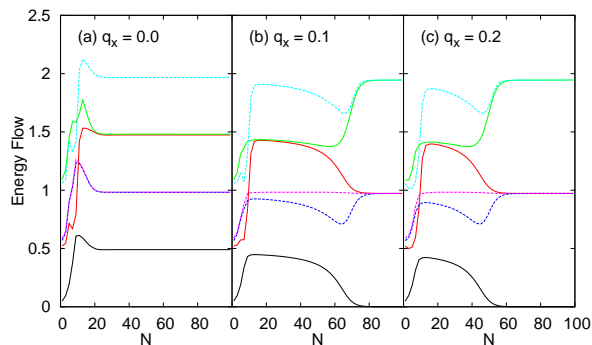


FIG. 3: (Color online) The NRG energy flows for the low-energy levels for Coulomb $U = 0.1$ with various drift momentum q_x . Solid lines: $(Q, S) = (1, 0)$, dashed lines: $(Q, S) = (0, 1/2)$.

state for non-zero repulsive U due to the marginal nature ($r = 1$) of the d -wave superconducting host. Here we calculate the energy flows as well as other physical quantities for fixed $U = 0.1$ and $V = 0.05$, with $q_y = 0$ and various q_x . As shown in Fig. 3, the NRG flows start and remain close to the free orbital (FO) regime at the high temperature or high energy. When lowering the temperature, two types of fixed points are identified. For the case with $q_x = 0$, the many-particle levels rapidly crossover to the LM fixed point from the FO regime. For the case with finite $q_x \neq 0$, the SC fixed point develops at sufficiently low temperatures. The evolution of energy flows from the LM lineshape to the SC one is similar to the soft-gap Anderson impurity model, implying that the impurity state is driven into the SC state by the current.

The IQPT is clearly manifested in some other physical quantities as illustrated in Fig. 4. The impurity spectral function develops a central peak at zero energy upon increasing q_x . This feature is similar to the soft-gap Anderson model where the impurity spectral function diverges at the zero energy for the SC and quantum critical phases.²² Remarkably, the sum rule is within 98% accuracy in our case. The IQPT is also indicated in the temperature dependence of the effective impurity moment and entropy, plotted in the inset of Fig. 4. It shows that the effective moment and entropy deviate from the free moment values ($0.25\mu_B$ and $\ln 2$ respectively) for $q_x = 0$ and approaches to zero for $q_x = 0.1$ and 0.2 . The later two cases indicate a SC phase where the impurity spin is completely screened at the low energy scale. We also calculated the finite temperature spectral function and found that in the SC phase the Kondo peak broadens with increasing temperatures and ultimately disappears at sufficiently higher temperatures due to thermal fluctuations.

The finite size effect, as detailed in Appendix B, prevents us from directly determining the precise location of the critical point q_x^c , below which the impurity is always in the localized state. To overcome this difficulty, we perform a scaling analysis on the critical behavior at

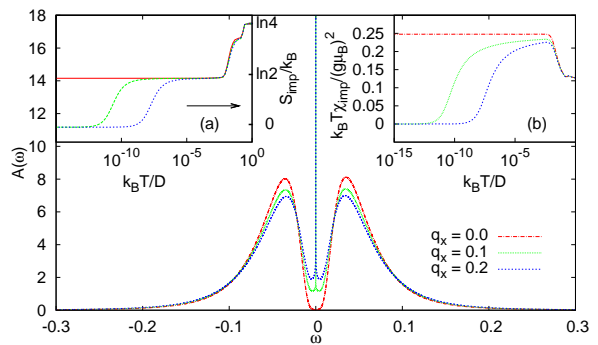


FIG. 4: (Color online) The impurity spectral function at $T = 0$ (main panel) and the temperature dependence of the effective impurity moment (right inset) and entropy (left) for Coulomb $U = 0.1$ with various q_x .

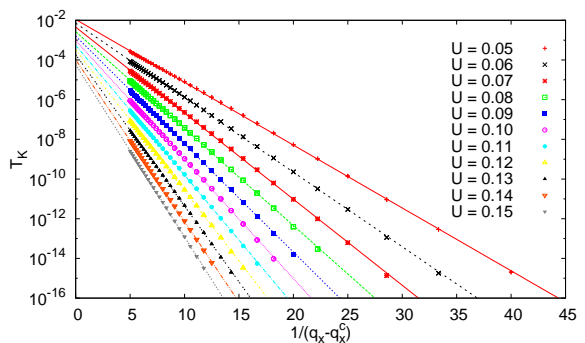


FIG. 5: (Color online) The Kondo temperature as a function of $1/(q_x - q_x^c)$ with various Coulomb interaction U . The fitting shows that the critical point $q_x^c \rightarrow 0$.

the zero temperature limit based on extensive calculations. We define an energy scale T_K , the Kondo temperature, around which the NRG flows crossover from the LM fixed point to SC fixed point. Specifically, for each value of $q_x > q_x^c$, the first excited many-particle energy level drops by 50% at T_K .²² T_K then follows a power-law or exponential behavior from the criticality, depending on whether it is a conventional continuous phase transition or a Kosterlitz-Thouless transition.²² As shown in Fig. 5, the Kosterlitz-Thouless type nature of the transition is clearly exhibited. The Kondo temperature T_K follows an exponential decay with the distance from the criticality, $\ln T_K = \ln T_0 - \alpha/(q_x - q_x^c)$, where T_0 and α are functions of U , independent on the current q_x . Also inferred from this fitting is that $q_x^c < 5.0 \times 10^{-3}$, much smaller than the scale of q_x (~ 0.1) used in our calculation. Hence the true location of q_x^c is vanishingly small as expected, implying $q_x^c \rightarrow 0$. The scaling analysis is free from the finite size effect since the residual DOS vanishes in the thermodynamic limit. The result therefore shows that $T_K = T_0 e^{-\alpha/q_x}$, where, as fitted in Fig. 6 for the small U -regime, α increases linearly with U , and T_0 decreases exponentially with increasing U .

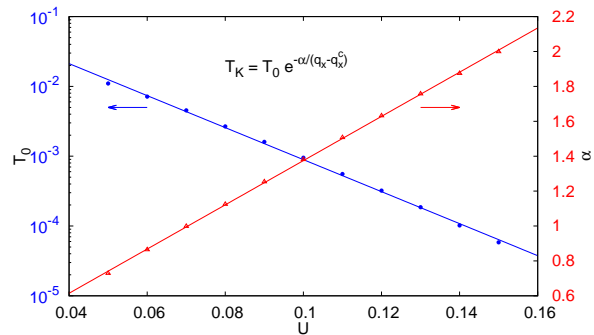


FIG. 6: (Color online) The fitting of Kondo temperature $T_K = T_0 e^{-\alpha/(q_x - q_x^c)}$, where $q_x^c \rightarrow 0$, T_0 and α are functions of Coulomb interaction U .

IV. CONCLUDING REMARKS

The results reported here explicitly show that the local impurity state is completely screened upon the non-zero (super-)current intensity while the impurity quantum criticality is in accordance with the well-known Kosterlitz-Thouless transition. Our findings have several implications: (i) In a d -wave superconductor, quasiparticle resonance can be induced around a doped static impurity in the strong scattering limit. Upon the flowing of a supercurrent, the resonance peak is suppressed in amplitude and broadened in width.²³ In contrast, for the quantum impurity as discussed here, a Kondo resonance emerges when it is driven into the SC phase by the supercurrent. This distinction of the response to the supercurrent can help us to decipher whether a doped atom plays the role of a static or quantum impurity in a d -wave superconductor. (ii) In high- T_c cuprates like $\text{Bi}_2\text{Sr}_2\text{CaCu}_2\text{O}_{8+\delta}$, the nanoscale inhomogeneity with the existence of small- and large-gap domains^{24,25} has been ubiquitously observed by the STM. When a magnetic impurity is doped into the system, it is in the LM phase in the absence of a supercurrent. In this case, the impurity plays the role of a weak potential scatter,²⁶ and the resonance as due to the quasiparticle scattering is located far away from the Fermi energy. This resonance should be observed in both types of domains. When a supercurrent flows in the sample, the impurities in the small-gap domains should be first driven into the SC phase and a Kondo resonance will emerge very close to the Fermi energy while those in the large-gap domains are still in the LM with no Kondo resonance. These interesting phenomena, which can be observed by STM, should serve as a direct test of our prediction.

We thank R. Bulla, X. Dai and T. Xiang for the technical helps and useful discussions. H.C., Y. W., and J.D. were supported by the NSF-China(No. 10934005, No. 10931160425), the NSF of Zhejiang Province(No. Z6110033), and the 973 Project of the MOST-China(No. 2010CB92300, No. 2009CB929104). J.-X.Z. was supported by the National Nuclear Security Administration

of the U.S. Department of Energy at LANL under Contract No. DE-AC52-06NA25396 and the U.S. DOE Office of Basic Energy Sciences. Part of numerical simulations were performed on a computer cluster at the Center for Integrated Nanotechnologies, a U.S. DOE Office of Basic Energy Sciences user facility.

- ¹ A.C. Hewson, *The Kondo Problem to Heavy Fermions*, (Cambridge University Press, Cambridge), 1993.
- ² K.G. Wilson, Rev. Mod. Phys. **47**, 773 (1975).
- ³ D. Withoff and E. Fradkin, Phys. Rev. Lett. **64**, 1835 (1990).
- ⁴ A.V. Balatsky, I. Vekhter, and J.-X. Zhu, Rev. Mod. Phys. **78**, 373 (2006).
- ⁵ A. Polkovnikov, S. Sachdev, and M. Vojta, Phys. Rev. Lett. **86**, 296 (2001).
- ⁶ J.-X. Zhu, C. S. Ting, and C.-R. Hu, Phys. Rev. B **62**, 6027 (2000).
- ⁷ A. Yazdani, B. A. Jones, C. P. Lutz, M. F. Crommie, and D. M. Eigler, Science **275**, 1767 (1997).
- ⁸ S. H. Pan, E. W. Hudson, K. M. Lang, H. Eisaki, S. Uchida, and J.C. Davis, Nature (London) **403**, 746 (2000).
- ⁹ T. Xiang, *The D-Wave Superconductors* (Science Press, Beijing, 2007).
- ¹⁰ J.-X. Zhu and Z. D. Wang, Phys. Rev. B **50**, 7207 (1994).
- ¹¹ P. D. de Gennes, *Superconductivity of Metals and Alloys* (W. A. Benjamin, Inc., New York, 1966).
- ¹² M. Vojta, Phil. Mag. **86**, 1807 (2006).
- ¹³ H.-J. Lee, R. Bulla, and M. Vojta, J. Phys.: Condens. Matter **17**, 6935 (2005).
- ¹⁴ Kan Chen and C. Jayaprakash, Phys. Rev. B **52**, 14436 (1995).
- ¹⁵ K. Ingersent, Phys. Rev. B **54**, 11936(1996); C. Gonzalez-Buxton and K. Ingersent, Phys. Rev. B **57**, 14254 (1998).
- ¹⁶ R. Bulla, T. Pruschke, and A.C. Hewson, J. Phys.: Condens. Matter, **12**, 4899 (1997).
- ¹⁷ The present model is also distinct from an Anderson impurity coupled to two s-wave superconducting leads where the IQPT is driven by varying the magnitude of the hard BCS gap and the phase difference of the two leads, see in C. Karrasch, A. Oguri, and V. Meden, Phys. Rev. B **77**, 024517 (2008).
- ¹⁸ H.R. Krishna-murthy, J.W. Wilkins, and K.G. Wilson, Phys. Rev. B **21**, 1003 (1980); **21**, 1044 (1980).
- ¹⁹ L. Fritz and M. Vojta, Phys. Rev. B **72**, 212510 (2005).
- ²⁰ M. Vojta and R. Bulla, Eur. Phys. J. B **28**, 283 (2002).
- ²¹ R. Bulla, T. Costi, and T. Pruschke, Rev. Mod. Phys. **80**, 395 (2008).
- ²² R. Bulla, N.N. Tong, and M. Vojta, Phys. Rev. Lett. **91**, 170601 (2003).
- ²³ D. Zhang, C. S. Ting, and C.-R. Hu, Phys. Rev. B **71**, 064521 (2005).
- ²⁴ S. H. Pan, J. P. O'Neal, R. L. Badzey, C. Chamon, H. Ding, J. R. Engelbrecht, Z. Wang, H. Eisaki, S. Uchida, A. K. Gupta, K.-W. Ng, E. W. Hudson, K. M. Lang, and J. C. Davis, Nature (London) **413**, 282 (2001).
- ²⁵ K. McElroy, Jinho Lee, J. A. Slezak, D.-H. Lee, H. Eisaki, S. Uchida, and J. C. Davis, Science **309**, 1048 (2005).
- ²⁶ M. Kircan, Phys. Rev. B **77**, 214508 (2008).

Appendix A: Local gauge transformation

A general BCS Hamiltonian can be written as

$$\mathcal{H}_{\text{BCS}} = - \sum_{ij,\sigma} t_{ij} \tilde{c}_{i\sigma}^\dagger \tilde{c}_{j\sigma} - \mu \sum_{i\sigma} \tilde{c}_{i\sigma}^\dagger \tilde{c}_{i\sigma} + \sum_{ij} \left[\tilde{\Delta}_{ij} \tilde{c}_{i\uparrow}^\dagger \tilde{c}_{j\downarrow} + \text{h.c.} \right]. \quad (\text{A1})$$

In the presence of a supercurrent as carried by paired electrons, the superconducting pair potential has the form

$$\tilde{\Delta}_{ij} = \Delta_{ij} \exp[i\mathbf{q} \cdot (\mathbf{r}_i + \mathbf{r}_j)], \quad (\text{A2})$$

where \mathbf{q} determines the center-of-mass motion of Cooper pairs¹¹.

Now we perform the local gauge transformation

$$c_{i\sigma} = \tilde{c}_{i\sigma} \exp[-i\mathbf{q} \cdot \mathbf{r}_i], \quad (\text{A3})$$

the BCS Hamiltonian is given by

$$\mathcal{H}_{\text{BCS}} = - \sum_{ij,\sigma} t_{ij} c_{i\sigma}^\dagger c_{j\sigma} e^{-i\mathbf{q} \cdot (\mathbf{r}_i - \mathbf{r}_j)} - \mu \sum_{i\sigma} c_{i\sigma}^\dagger c_{i\sigma} + \sum_{ij} \left[\Delta_{ij} c_{i\uparrow}^\dagger c_{j\downarrow} + \text{h.c.} \right]. \quad (\text{A4})$$

We then introduce the Fourier transform to cast the BCS Hamiltonian into the momentum representation,

$$c_{i\sigma} = \frac{1}{\sqrt{N_L}} \sum_{\mathbf{k}} c_{\mathbf{k}\sigma} \exp[i\mathbf{k} \cdot \mathbf{r}_i], \quad (\text{A5})$$

where N_L is the number of lattice sites. A straightforward algebra yields

$$\mathcal{H}_{\text{BCS}} = \sum_{\mathbf{k},\sigma} \xi_{\mathbf{k}+\mathbf{q}} c_{\mathbf{k}\sigma}^\dagger c_{\mathbf{k}\sigma} + \sum_{\mathbf{k}} [\Delta_{\mathbf{k}} c_{\mathbf{k}\uparrow}^\dagger c_{-\mathbf{k}\downarrow}^\dagger + \text{h.c.}]. \quad (\text{A6})$$

This is equivalent to Eq.(1) of the main text in the absence of the magnetic impurity. In the tight-binding approximation, the conduction electrons have the normal and d -wave superconducting gap dispersions, $\xi_{\mathbf{k}} = -2t(\cos k_x + \cos k_y) - 4t' \cos k_x \cos k_y - \mu$ and $\Delta_{\mathbf{k}} = (\Delta_0/2)(\cos k_x - \cos k_y)$, respectively. Thus we demonstrated that the single particle energy picks up a momentum \mathbf{q} -shift from the order parameter. It reflects a fundamental fact that the superconducting Cooper is formed by two electrons in the presence of an effective pairing interaction. The quasiparticle spectrum

$$E_{\mathbf{k},\mathbf{q}}^\pm = \frac{\xi_{\mathbf{k}+\mathbf{q}} - \xi_{\mathbf{k}-\mathbf{q}}}{2} \pm \sqrt{\left(\frac{\xi_{\mathbf{k}+\mathbf{q}} + \xi_{\mathbf{k}-\mathbf{q}}}{2} \right)^2 + \Delta_{\mathbf{k}}^2} \quad (\text{A7})$$

is easily obtained by diagonalizing the BCS Hamiltonian through a canonical transformation. It fully agrees with

the expression given in the de Gennes's book.¹¹ The same quasiparticle energy dispersion $E_{\mathbf{k},\mathbf{q}}^{\pm}$, together with $\xi_{\mathbf{k}}$ and $\Delta_{\mathbf{k}}$, are also given in the main text.

We emphasize that in the presence of the superconducting order parameter, the current \mathbf{q} introduced in the expression of the single particle spectrum is the supercurrent, while it is a normal state current in the absence of the superconducting order parameter. This natural recovery merely shows the correctness of the formalism. Therefore, the supercurrent can tune the quasiparticle spectrum and density of states in a non-trivial way, which in turn result in significant consequences on the quantum impurity state in an unconventional superconducting medium as studied in the main text of this paper.

Appendix B: The finite size analysis

The conduction electron DOS of the bulk system is obtained by numerical calculation for a relatively large but still finite lattice system. There is unavoidably a residual DOS in the absence of transport current due to the finite size effect. Since the NRG can resolve exponentially small energies and temperatures, the residual DOS at the Fermi level for the $q_x = 0$ case remains a challenging problem in the finite lattice size calculation and should be treated with caution. The situation is in contrast to the conventional Anderson impurity model with

a known soft-gap where the analytical expression of the DOS is available.

Therefore, we shall clarify how the residual DOS for the $q_x = 0$ case varies with the system size. We first performed a scaling analysis on the size dependent DOS. To ensure a sufficiently smooth density of states, we set the broadening parameter $\Gamma \propto 2^{-L}$ in numerical calculations. In the thermodynamic limit, the intrinsic lifetime parameter $\Gamma \rightarrow 0^+$ is recovered. As shown in Fig. 7, the residual DOS in the absence of the current becomes very smaller and approaches zero if we increase the system size up to $2^{16} \times 2^{16}$, while the DOS at the Fermi level for $q_x = 0.1$ and 0.2 is almost size independent. This feature makes our results based on finite current reliable and robust.

We then proceed to differentiate the low energy behavior, which may suffer from the finite size effect for a very small q_x . For this purpose we compare the NRG energy flows for the cases with $q_x = 0$ and 0.01 , respectively. As shown in Fig. 8, the LM fixed point is stable up to the maximal iteration $N_{\max} = 100$ for $q_x = 0$, while it reveals unstable signals (though being tiny) for very small current $q_x = 0.01$. This provides strong evidence that the residual DOS at the Fermi level is negligible when the current is turned on. Hence the scaling behavior of the Kondo temperature T_K with the finite current investigated in the main text reveals the correct physics for $q_x \rightarrow 0$.

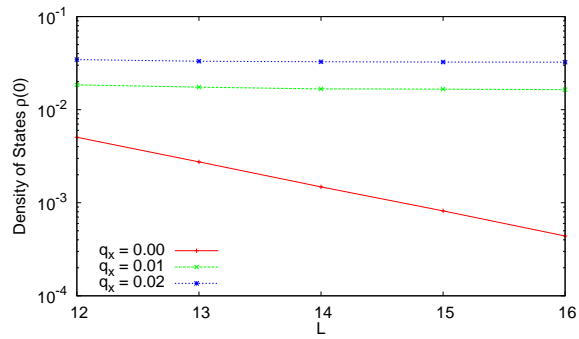


FIG. 7: (Color online) The DOS at the Fermi level as a function of L with the system size $N_L = 2^L \times 2^L$.

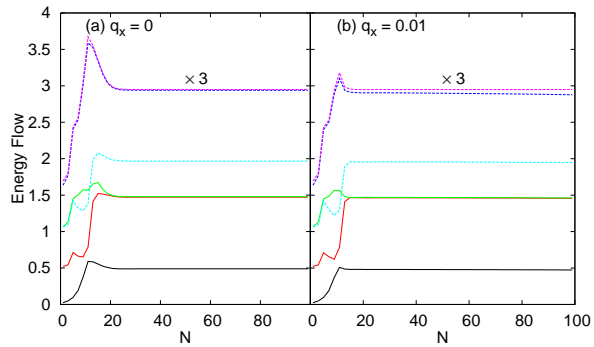


FIG. 8: (Color online) The NRG energy flows for the low-energy levels for Coulomb $U = 0.05$ with $q_x = 0$ and 0.01 . Solid lines: $(Q, S) = (1, 0)$, dashed lines: $(Q, S) = (0, 1/2)$.